Analytical expressions for the fourth virial coefficient of a hard-sphere mixture

Stanislav Labík[*] and Jiří Kolafa[†]

Department of Physical Chemistry, Institute of Chemical Technology, 166 28 Prague 6, Czech Republic
(Received 26 August 2009; published 23 November 2009)

A method of numerical calculation of the fourth virial coefficients of the mixture of additive hard spheres is proposed. The results are compared with an exact analytical formula for the fourth partial virial coefficient $B_4^{[1]}$ (i.e., three spheres of diameters σ_1 and one sphere of diameter σ_2) and a semiempirical expression for $B_4^{[2]}$ (i.e., two spheres of each kind). It is shown that the first formula is nonanalytic and the implication to the equations of state for hard-sphere mixtures is discussed.

I. INTRODUCTION

A common starting point for the equation of state of the hard-sphere (HS) fluid is the known virial series. The virial expansion in powers of density for the fluid is

$$z = 1 + \sum_{n=2}^{\infty} B_n \rho^{n-1}, \tag{1}$$

where $z = pV/(Nk_BT)$, k_B is the Boltzmann constant, B_n are the virial coefficients and ρ is the number density, $\rho = N/V$. The virial coefficients are defined by exact formulas (free from any approximation) in terms of integrals whose integrands depend on intermolecular potential energy [1,2].

In principle, the virial coefficients can be calculated for any order. Unfortunately, calculation of high-order coefficients becomes increasingly difficult because both the number of integrals and their dimensionality rapidly increase. For the pure HS system only the second, third, and fourth virial coefficients are known analytically. It holds [3,4]

$$B_2 = \frac{2\pi}{3}, \quad B_3 = \frac{5\pi^2}{18},$$

$$B_4 = \left(\frac{\pi}{6}\right)^3 \frac{2707\pi + 438\sqrt{2} - 4131\arccos(1/3)}{70\pi}, \tag{2}$$

where we take the sphere diameter, σ, as a unit of length. The higher virial coefficients up to B_{10} were obtained by a numerical integration [5–16].

The virial coefficients for a hard-sphere mixture are composition dependent. For a binary mixture it holds

$$B_n(s) = \sum_{i=0}^{2} \binom{n}{i} B_n^{[i]}(s) x_1^{n-i} x_2^i \tag{3}$$

where x_1 and x_2 are the molar fractions of particles 1 and 2, respectively. Throughout the paper we take the first diameter of the spheres, σ_1, as a unit of length. Then the partial virial coefficients, $B_n^{[i]}(s)$, depend on the diameter ratio $s = \sigma_2/\sigma_1$. Up to now only the second and third virial coefficients have been known exactly [17,18]

$$B_2^{[0]}(s) = \frac{2\pi}{3}, \quad B_2^{[1]}(s) = \frac{2\pi}{3}\left(\frac{1+s}{2}\right)^3, \quad B_2^{[2]}(s) = \frac{2\pi}{3}s^3, \tag{4}$$

and

$$B_3^{[0]}(s) = \frac{5\pi^2}{18}, \tag{5a}$$

$$B_3^{[1]}(s) = \frac{\pi^2}{108}(1 + 6s + 15s^2 + 8s^3), \tag{5b}$$

$$B_3^{[2]}(s) = \frac{\pi^2 s^3}{108}(8 + 15s + 6s^2 + s^3), \tag{5c}$$

$$B_3^{[3]}(s) = \frac{5\pi^2}{18}s^6. \tag{5d}$$

For $B_4(s)$, only $B_4^{[0]}(s)$ and $B_4^{[4]}(s)$ corresponding to the pure HS are known analytically. An analytical expression for $B_4^{[1]}$ was found at small diameter ratio, $s < 2/\sqrt{3} - 1 \doteq 0.1547$ [19],

$$B_4^{[1]}(s) = \left(\frac{\pi}{6}\right)^3 \left[-\frac{9}{56}s^9 - \frac{81}{56}s^8 - \frac{162}{35}s^7 - \frac{27}{5}s^6 + \frac{27}{40}s^5 \right.$$
$$\left. + \frac{27}{8}s^4 + \frac{21}{4}s^3 + 9s^2 + \frac{9}{4}s + \frac{1}{4} \right] \tag{6}$$

and due to symmetry condition

$$B_4^{[i]}(s) = s^9 B_4^{[n-i]}(1/s), \tag{7}$$

we can also obtain $B_4^{[3]}(s)$ for $s > \sqrt{3}/(2-\sqrt{3}) \doteq 6.464$. An exact expression for other diameter ratios and the whole s range of $B_4^{[2]}(s)$ is unknown and only numerical values are available [20,21]. The numerical values are also known for the higher virial coefficients up to $B_7(s)$ [14,20,22].

The aim of this work is to propose a numerical method for the calculation of $B_4(s)$ for a HS mixture. We also find an exact analytical expression for $B_4^{[1]}(s)$ and $B_4^{[3]}(s)$ and a very accurate semiempirical expression for $B_4^{[2]}(s)$. On the basis of these findings we can explain why different empirical equations of state based on extended scaled particle theory have had only moderate success.

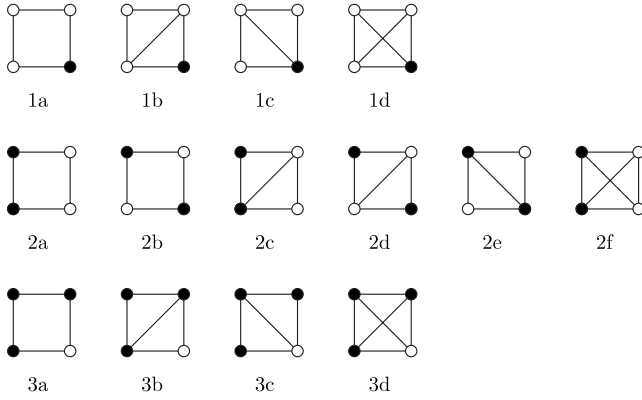*stanislav.labik@vscht.cz
†jiri.kolafa@vscht.cz

FIG. 1. The diagrams representing the topologically different groups of contributions to the partial virial coefficients. Open and filled circles represent components 1 (with diameters $\sigma_1 = 1$) and 2 (with diameters of $\sigma_2 = s$), respectively.

II. NUMERICAL CALCULATIONS

A. Basic formulas

The fourth partial virial coefficient of a HS mixture is given by the sum of all cluster integrals corresponding to labeled irreducible f-bond diagrams with four colored points [23].

$$B_4^{[1]}(s) = 3B_4^{[1a]}(s) + 3B_4^{[1b]}(s) + 3B_4^{[1c]}(s) + B_4^{[1d]}(s),$$
(8a)

$$B_4^{[2]}(s) = 2B_4^{[2a]}(s) + B_4^{[2b]}(s) + 4B_4^{[2c]}(s) + B_4^{[2d]}(s) + B_4^{[2e]}(s) + B_4^{[2f]}(s),$$
(8b)

$$B_4^{[3]}(s) = 3B_4^{[3a]}(s) + 3B_4^{[3b]}(s) + 3B_4^{[3c]}(s) + B_4^{[3d]}(s),$$
(8c)

where $B_4^{[ij]}(s)$ are contributions to the partial virial coefficients by topologically different groups of coefficients (see Fig. 1).For example, the coefficient $B_4^{[2f]}(s)$ is

$$B_4^{[2f]}(s) = -\frac{1}{8}\int\int\int f_{12}f_{13}f_{23}f_{14}f_{24}f_{34}d\mathbf{r}_2 d\mathbf{r}_3 d\mathbf{r}_4,$$
(9)

where function f_{ij} is the Mayer function, which is either -1 if the particles overlap or 0 if they do not, the open circles correspond to hard spheres with diameters $\sigma_1 = 1$ and the filled circles to hard spheres with $\sigma_2 = s$.

All contributions in Eq. (8) can be calculated analytically using the three-dimensional (3D) Fourier transform and convolution (see Appendix). The only exceptions are the last contributions to each partial virial coefficient corresponding to the two-irreducible diagram. They can be calculated by some numerical integration. In previous papers a Monte Carlo (MC) integration technique was used [23]. In this method, a chain of four overlapping spheres is randomly created and the value of a two-irreducible diagram is obtained from the probability that remaining three f bonds are also satisfied. The uncertainty of the results decreases with

the square root of the number of generated chains. Enormously long calculations would by necessary to reach very precise results.

B. Method

To simplify calculations of two-irreducible contributions we can rewrite Eq. (9) to separate the integration over a position of the fourth particle. Equation (9) then becomes

$$B_4^{[2f]}(s) = -\frac{1}{8}\int\int f_{12}f_{13}f_{23}\times\left[\int f_{14}f_{24}f_{34}d\mathbf{r}_4\right]d\mathbf{r}_2 d\mathbf{r}_3.$$
(10)

The integrand of the integral in the brackets is not zero, if the fourth sphere overlaps with the others. It means that the center of the fourth sphere (with diameter s) must lie in the overlap of the excluded regions of the three other spheres. The term "excluded region of a hard body" is used as an abbreviation of the more exact but much longer term "the region in which the center of the additional sphere cannot be located without overlapping the body and the additional sphere." Then Eq. (10) becomes

$$B_4^{[2f]}(s) = \frac{1}{8}\int\int f_{12}f_{13}f_{23}V_{\text{exc}}^{[3]}(\mathbf{r}_2,\mathbf{r}_3)d\mathbf{r}_2 d\mathbf{r}_3,$$
(11)

where $V_{\text{exc}}^{[3]}(\mathbf{r}_2,\mathbf{r}_3)$ is the volume of intersection of the excluded regions of spheres 1, 2, and 3. If spheres 1 and 2 have diameter 1 and spheres 3 and 4 diameter $s < 1$, the integration may be simplified using the polar and bispherical coordinate systems giving

$$B_4^{[2f]}(s) = \pi^2\int_0^{(1+s)/2}\int_0^{(1+s)/2}\int_{|a-b|}^{a+b}f(c)$$
$$\times V^{[3]}(a,b,c)abc\,dc\,db\,da,$$
(12)

where a, b, and c are the distances between centers of spheres 2–3, 1–3, and 1–2, respectively. Three different cases may occur as seen in Fig. 2. In Fig. 2(a), the excluded region of the third sphere is fully contained in the excluded regions of both spheres 1 and 2. The intersection of the excluded regions is then identical to the excluded region of the third particle and

$$V_{\text{exc}}^{[3]}(a,b,c) = \frac{4\pi}{3}s^3.$$
(13)

In Fig. 2(b), the excluded region of the third sphere is fully contained in the excluded region of the first sphere only. The
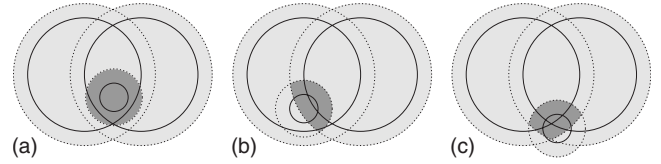

FIG. 2. Three different configurations of excluded regions of hard spheres. The light shadow areas correspond to the excluded regions of spheres and the dark shadow area to their intersection.

TABLE I. The partial virial coefficients for different diameter ratios.

s	$B_4^{[1]}(s)$	$B_4^{[2]}(s)$	$B_4^{[3]}(s)$
0.05	$5.5363065926 \times 10^{-2}$	$4.2899720643 \times 10^{-5}$	$1.7748605793 \times 10^{-8}$
0.10	$8.1906578467 \times 10^{-2}$	$4.0408838130 \times 10^{-4}$	$1.1970915337 \times 10^{-6}$
0.15	$1.1618867322 \times 10^{-1}$	$1.5866001798 \times 10^{-3}$	$1.4353978244 \times 10^{-5}$
0.20	$1.5893702101 \times 10^{-1}$	$4.3324295186 \times 10^{-3}$	$8.4807580777 \times 10^{-5}$
0.25	$2.1091252409 \times 10^{-1}$	$9.6676440221 \times 10^{-3}$	$3.3984081090 \times 10^{-4}$
0.30	$2.7289168283 \times 10^{-1}$	$1.8951505010 \times 10^{-2}$	$1.0649087420 \times 10^{-3}$
0.35	$3.4565959608 \times 10^{-1}$	$3.3929371019 \times 10^{-2}$	$2.8153238544 \times 10^{-3}$
0.40	$4.3000682538 \times 10^{-1}$	$5.6789237081 \times 10^{-2}$	$6.5707917903 \times 10^{-3}$
0.45	$5.2672765878 \times 10^{-1}$	$9.0221808911 \times 10^{-2}$	$1.3940836203 \times 10^{-2}$
0.50	$6.3661904860 \times 10^{-1}$	$1.3748404068 \times 10^{-1}$	$2.7429837490 \times 10^{-2}$
0.55	$7.6047991830 \times 10^{-1}$	$2.0246608476 \times 10^{-1}$	$5.0771118596 \times 10^{-2}$
0.60	$8.9911068887 \times 10^{-1}$	$2.8976161505 \times 10^{-1}$	$8.9340242203 \times 10^{-2}$
0.65	1.0533129434	$4.0474149532 \times 10^{-1}$	$1.5065843807 \times 10^{-1}$
0.70	1.2238891830	$5.5363077020 \times 10^{-1}$	$2.4499785734 \times 10^{-1}$
0.75	1.4116426444	$7.4358896209 \times 10^{-1}$	$3.8610115252 \times 10^{-1}$
0.80	1.6173771622	$9.8279366024 \times 10^{-1}$	$5.9202870779 \times 10^{-1}$
0.85	1.8418970610	1.2805273917	$8.8614769544 \times 10^{-1}$
0.90	2.0860070726	1.6472677654	1.2982780073
0.95	2.3505122685	2.0947808824	1.8660110114

volume $V_{\text{exc}}^{[3]}$ is then equal to the volume of intersection of excluded regions of the second and third spheres,

$$
V_{\text{exc}}^{[3]}(a,b,c) = \frac{\pi}{12a}\left[a^2 + (1+3s)a - \frac{3}{4}(1-s)^2 \right]
$$
$$
\times \left[a - \frac{1}{2}(1+3s) \right]^2. \tag{14}
$$

The same relation holds if the excluded volume of the third sphere is contained in the excluded region of the second sphere with a substituted by b, i.e., the distance between centers of the spheres 1 and 3. In Fig. 2(c), the volume $V_{\text{exc}}^{[3]}$ is given by the intersection of all three excluded regions. The expression for the triple intersection can be found in [24] with a small correction pointed out in [25].

The integration of Eq. (12) was carried out analytically in regions where Eqs. (13) and (14) are valid, and numerically for the triple intersection. We used a code which combines the separation of the integration ranges into regions where the integrand is a smooth function, Simpson's quadrature rule and extension of the Romberg extrapolation procedure. The calculation of a single value on a regular PC takes only several minutes.

For the remaining two-irreducible diagrams we used a similar procedure. The complete partial virial coefficients were obtained using Eq. (8). The final results are listed in Table I. The estimated relative uncertainty is less then 10^{-10}.

Our results are compared with the best literature data [21] in Fig. 3. The relative differences between both data sets are smaller than the uncertainty of the literature data with the exception of two points for $B_4^{[2]}$ where the differences are two times greater. The estimated uncertainty of our data is of

course roughly million times smaller. Validity of our data has been confirmed by comparison with the analytical formulas presented in the next section.

III. ANALYTICAL FORMULAS

A. Partial virial coefficients $B_4^{[1]}(s)$ and $B_4^{[2]}(s)$

The dimensionless chemical potential of the infinitely diluted hard sphere is obtained from Eqs. (1) and (3) using a standard thermodynamic route giving
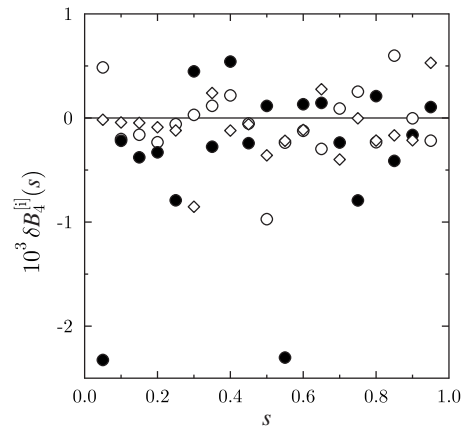

FIG. 3. The relative difference of the literature data and the new values of the partial virial coefficients for different diameter ratios. White circles, full circles and diamonds correspond to $B_4^{[1]}(s)$, $B_4^{[2]}(s)$ and $B_4^{[3]}(s)$, respectively.

$$\beta\mu_1^\infty(s) = \sum_{n=2}^\infty \frac{n}{n-1} B_n^{[1]}(s)\rho^{n-1}, \tag{15}$$

where $\mu_1^\infty(s)$ is the residual chemical potential of an infinitely diluted hard sphere of diameter s in the system of spheres od diameter 1 and $\beta = 1/(k_B T)$.

The same chemical potential is related to the average probability of creating a cavity of diameter s in the *NVT* ensemble, $P(s)$ [26],

$$\beta\mu_1^\infty(s) = -\ln[P(s)]. \tag{16}$$

At limit $s = 0$ this probability is related to the ratio of the intrinsic volume of molecules and the volume of the system giving

$$P(0) = 1 - \frac{\pi}{6}\rho. \tag{17}$$

Using the Taylor series in density we get from Eqs. (15)–(17)

$$B_n^{[1]}(0) = \frac{1}{n}\left(\frac{\pi}{6}\right)^{n-1}. \tag{18}$$

Differentiation of Eq. (16) with respect to s gives [26–28]

$$\frac{\mathrm{d}\beta\mu_1^\infty(s)}{\mathrm{d}s} = \frac{\pi}{2}(1+s)^2\rho g_2^\infty(s), \tag{19}$$

where $g_2^\infty(s)$ is the contact distribution function of the pair of molecules with diameters 1 and s at infinite dilution.

For small densities the zeroth order approximation

$$g_2^\infty(s) = 1 \tag{20}$$

together with Eqs. (15)–(17) give the exact expression for $B_2^{[1]}(s)$.

Some time ago, we showed [26] that $g_2^\infty(s)$ is related to the thermodynamic properties by

$$\ln[g_2^\infty(s)] = \beta\mu_1^\infty(s) + \beta\mu_1(1) - \beta\mu_2^\infty(1,s), \tag{21}$$

where $\mu_1(1)$ is the chemical potential of the pure HS system and $\mu_2^\infty(1,s)$ is the chemical potential at infinite dilution of a hard dumbbell formed by a pair of spheres with diameter 1 and s at contact. The second and third term of the right hand side of Eq. (21) can be joined giving

$$\ln[g_2^\infty(s)] = \beta\mu_1(1) - \beta w_2^\infty(s), \tag{22}$$

where $w_2^\infty(s)$ is the work needed to form a cavity of diameter s at contact with a HS of diameter 1. It can be expressed as

$$\beta w_2^\infty(s) = \frac{\pi}{4}\rho\int_0^s (1+x)^2 \int_{\cos\theta^\star}^1 (1+\cos\theta)$$
$$\times g_3^\infty(x,\theta)\mathrm{d}\cos\theta\mathrm{d}x, \tag{23}$$

where $g_3^\infty(x,\theta)$ is the distribution function of the HS at contact with the hard dumbbell formed by two touching HS of diameters 1 and x, θ is the angle between the joins of centers of spheres as shown in Fig. 4. The lower limit of the second integral
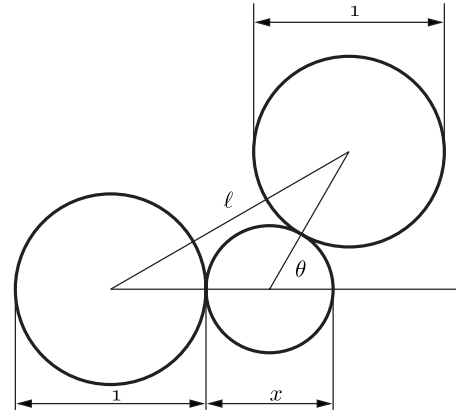

FIG. 4. The configuration of three hard spheres at contact.

$$\cos\theta^\star = \frac{1 - 2x - x^2}{(1+x)^2} \tag{24}$$

corresponds to the configuration, in which all three spheres are at contact. Equation (23) can be simplified using substitution $\ell^2 = (1+x)^2(1+\cos\theta)$

$$\beta w_2^\infty(s) = 2\pi\rho\int_0^s \frac{1}{(1+x)^2}\int_1^{1+x} \ell^3 g_3^\infty(x,\ell)\mathrm{d}\ell\mathrm{d}x, \tag{25}$$

where ℓ is the distance between both hard spheres of diameter 1.

From $g_3^\infty(x,\ell) = 1$ we get the first-order approximation. It gives

$$g_2^\infty(s) = 1 + \frac{\pi}{6}\frac{1+4s}{1+s}\rho + \dots, \tag{26}$$

where the coefficient of ρ has a geometrical meaning as the volume of the intersection of excluded regions of both spheres. The first order approximation with Eqs. (15)–(17) gives the exact expression for both $B_2^{[1]}(s)$ and $B_3^{[1]}(s)$.

The second order approximation can be obtained in a similar way. The distribution function $g_3^\infty(x,\ell)$ is approximated by

$$g_3^\infty(x,\ell) = 1 + \Delta V_{\mathrm{exc}}^\star(x,\ell)\rho, \tag{27}$$

where $\Delta V_{\mathrm{exc}}^\star(x,\ell)$ is the intersection of the excluded regions of a dumbbell (formed by touching spheres of diameters 1 and x) and a sphere at contact with the smaller sphere as shown in Fig. 5.

Two different situations may occur. In Fig. 5(a), the cavity B is small and its excluded region is fully contained in the union of the excluded regions of both spheres A and C. The volume of the intersection of the excluded regions is given by

$$\Delta V_{\mathrm{exc}}^\star(x,\ell) = \Delta V_{\mathrm{exc}}^{[1]}[B] + \Delta V_{\mathrm{exc}}^{[2]}[A,C] - \Delta V_{\mathrm{exc}}^{[2]}[A,B], \tag{28}$$

where $\Delta V_{\mathrm{exc}}^{[1]}[B]$ is the excluded volume of cavity B and $\Delta V_{\mathrm{exc}}^{[2]}[I,J]$ is the volume of the intersection of excluded regions of spheres I and J. In Fig. 5(b), the excluded region of B is not fully contained in the union of intersections and
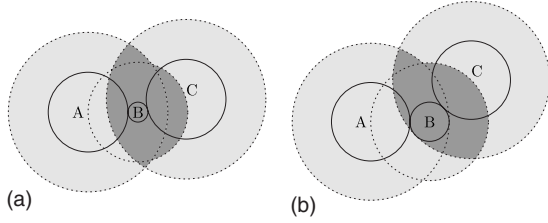
FIG. 5. Two types of the intersection of excluded regions of hard spheres. The light shadow areas correspond to the excluded regions of hard dumbbell and sphere and the dark shadow area to their intersection. Hard spheres A and C have diameters 1 and the cavity B has diameter $x < 1$

$$\Delta V_{\text{exc}}^{\star}(x, \ell) = \Delta V_{\text{exc}}^{[2]}[A, C] + \Delta V_{\text{exc}}^{[2]}[B, C] - \Delta V_{\text{exc}}^{[3]}[A, B, C], \quad (29)$$

where $\Delta V_{\text{exc}}^{[3]}[A, B, C]$ is the volume of the intersection of excluded regions of spheres A, B and C. We remark that the difference between Eqs. (28) and (29) equals the portion of the excluded volume of B which is not contained in the intersection of the excluded regions of A and C. The volumes

of the pair intersections are obtained as a difference of volumes of the spheres and the dumbbell, and the volume of the triple intersection is given by formulas in [24,25].

For small values of s, $s < 2/\sqrt{3} - 1$, the situation illustrated in Fig. 5(a) occurs in all configurations giving

$$\Delta V_{\text{exc}}^{\star}(x, \ell) = \pi \left[\frac{\ell^3}{12} - \ell + \frac{(x^2 + 2)(x + 2)^2}{6(1 + x)} \right] \quad (30)$$

and the integrations in Eq. (25) yield

$$\beta w_2^{\infty}(s) = \frac{\pi s^2 \rho}{6} \frac{s^2 + 4s + 6}{1 + s} + \frac{\pi^2 s^2 \rho^2}{2520}(1 + s)^2(1050 + 1120s + 980s^2 + 1288s^3 + 1008s^4 + 360s^5 + 45s^6). \quad (31)$$

Combining it with Eqs. (15)–(17) reproduces the exact expression for $B_4^{[1]}(s)$ given by Eq. (6).

For $s > 2/\sqrt{3} - 1$, the calculation of $w_2^{\infty}(s)$ is substantially more complicated and it was obtained by a very careful usage of the computer algebraic system Maple [29]. The integrals in Eq. (25) cannot be obtained by the automatic integration routine built in but needs a lot of human intervention. The final results are given by Eq. (6) plus the additional term

$$\Delta B_4^{[1]}(s) = \pi^2 \left[\frac{1}{8} s(s + 2)P_1 - \frac{79}{1120} s(s + 2)P_2 - \frac{1}{960} s^2(3s^3 + 15s^2 + 25s + 15)P_3 - \frac{17}{2240} s(s^2 + 3s + 3)P_4 \right.$$

$$- \frac{1}{2240}(17s^3 + 51s^2 + 51s - 144)P_5 - \frac{1}{6720} s(5s^8 + 45s^7 + 144s^6 + 168s^5 + 279s^2 + 261s - 630)P_6 - \frac{3}{35} s(s + 2)P_7$$

$$- \frac{11}{280} s(s + 2)P_8 - \frac{1}{960} s(3s^4 + 15s^3 + 25s^2 + 15s - 90)P_9 + \frac{1}{13440} s^2(5s^7 + 45s^6 + 144s^5 + 168s^4 + 279s + 261)P_{10}$$

$$+ \frac{\pi}{13440}(10s^9 + 90s^8 + 288s^7 + 336s^6 - 21s^5 - 105s^4 + 383s^3 + 729s^2 + 624s - 432)$$

$$\left. + \frac{Q}{80640}(30s^6 + 180s^5 + 279s^4 - 84s^3 - 210s^2 + 228s + 745) \right], \quad (32)$$

where

$$P_1 = \arctan\left(\frac{Q}{2}\right),$$

$$P_2 = \arctan(Q),$$

$$P_3 = \arctan\left(\frac{Q}{1 + s}\right),$$

$$P_4 = \arctan\left(\frac{-1 + 3s}{Q}\right),$$

$$P_5 = \arctan\left(\frac{7 + 3s}{Q}\right),$$

$$P_6 = \arctan\left(\frac{1 + s}{Q}\right),$$

$$P_7 = \arctan\left(\frac{1 + 3s^2 + 6s}{Q}\right),$$

$$P_8 = \arctan\left(\frac{-1 + 2s + s^2}{Q}\right),$$

$$P_9 = \arctan\left[\frac{-1 + 2s + s^2}{(1 + s)Q}\right],$$

$$P_{10} = \begin{cases} \arctan\left[\dfrac{Q(1+s)(-1+2s+s^2)}{s^4+4s^3+6s^2+4s-1}\right] - \pi & s < 2^{1/4} \\ -\pi/2 & s = 2^{1/4} \\ \arctan\left[\dfrac{Q(1+s)(-1+2s+s^2)}{s^4+4s^3+6s^2+4s-1}\right] & s > 2^{1/4} \end{cases},$$

$$Q = \sqrt{3s^2+6s-1}.$$

It means that $B_4^{[1]}(s)$ is not an analytic function at $s_0 = 2/\sqrt{3} - 1$. For $s < s_0$ the additional term, $\Delta B_4^{[1]}$, is zero, and for s slightly greater than s_0 it can be expanded to

$$\Delta B_4^{[1]} = \frac{\pi^2 \sqrt[4]{3}\,\Delta s^{11/2}}{216}\left(\frac{7776}{385}\sqrt{3} - \frac{2916}{5005}\Delta s \right.$$
$$\left. + \frac{4481163}{100100}\sqrt{3}\,\Delta s^2 + \cdots\right), \qquad (33)$$

where $\Delta s = s - s_0$. It implies that $B_4^{[1]}(s)$ has a discontinuity in the sixth derivative at s_0.

Equation (32) was derived for $s < 1$ only but a similar analysis for $s > 1$ has shown that the same formula is also valid in this range.

To verify the final results given by Eqs. (6) and (32) several tests were performed. The limiting behavior at small values of s and the asymptotic expansion at big values of s discussed in details in [30] is fully reproduced. For $s = 1$ the formulas simplify to the pure HS formula given by Eq. (2). As the derivative of the residual excess free energy of mixing with respect to s must be zero when $s = 1$, the derivative of the partial virial coefficients must satisfy condition [31]

$$\left[\frac{dB_n^{(m)}(s)}{ds}\right]_{s=1} = \frac{3(n-1)m}{n}B_n. \qquad (34)$$

This condition is also exactly fulfilled.

The values of $B_4^{[1]}(s)$ for $s < 1$ and $B_4^{[3]}(s)$ obtained at the same range from the symmetry condition Eq. (7) were compared with the results of the numerical method described in the previous section in Fig. 6. It is seen that the results coincide with relative deviations to better than 1×10^{-10}.

B. Partial virial coefficients $B_4^{[2]}(s)$

We do not have an analytical formula for the partial virial coefficients $B_4^{[2]}(s)$. On the other hand, there are a lot of conditions enabling to find a precise empirical expression in the whole range $s \in [0, \infty]$.

All terms of $B_4^{[2]}(s)$ in Eq. (8b) but the last one, corresponding to the two-irreducible diagram, are known analytically. At small diameter ratio, s, the contribution due to the two-irreducible diagram, $B_4^{[2f]}(s)$, is nearly the same as the negative value of the contribution $B_4^{[2e]}(s)$. The corresponding diagrams differ in a single f bond connecting two spheres with diameters 1. The conditional probability that both big spheres overlap, provided that all other pairs of spheres overlap, is nearly one. The comparison of the values of numerical calculation of $B_4^{[2f]}(s)$ and the analytical formula for $B_4^{[2e]}(s)$ from Appendix shows that both contributions have the same
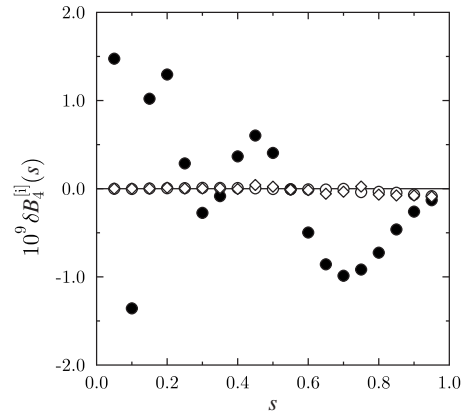

FIG. 6. The relative difference of the numerical values and analytical formulas of the partial virial coefficients for different diameter ratios. The white circles, full circles and diamonds correspond to $B_4^{[1]}(s)$, $B_4^{[2]}(s)$, and $B_4^{[3]}(s)$, respectively.

first three terms in the Maclaurin series and differ only in sign

$$B_4^{[2f]}(s) \approx -B_4^{[2e]}(s) = -\left(\frac{\pi}{6}s\right)^3\left(1 + \frac{15}{4}s + \frac{51}{10}s^2 + \cdots\right). \qquad (35)$$

At $s = 1$ we have two other conditions. The partial virial coefficients $B_4^{[2]}(s)$ must reduce to the fourth virial coefficient of pure HS

$$B_4^{[2]}(1) = B_4 \qquad (36)$$

and the consistency condition Eq. (34) gives

$$\left[\frac{dB_4^{(2)}(s)}{ds}\right]_{s=1} = \frac{9}{2}B_4. \qquad (37)$$

For $s > 1$ the symmetry condition given by Eq. (7) applies. It reduces to the relation

$$B_4^{[2]}(s) = s^9 B_4^{[2]}(1/s), \qquad (38)$$

which together with Eq. (35) gives the asymptotic behavior for big s.

To fulfill all conditions, the following semiempirical formula for $B_4^{[2]}(s)$ was proposed

$$B_4^{[2]}(s) = \frac{\pi^3 s^3}{288}(1+s)(4+11s+4s^2) + B_4^{[2f]}(s) \qquad (39)$$

and

$$B_4^{[2f]}(s) = -\frac{\pi^3 s^{9/2}}{216}\left[\sqrt{2}\left(\frac{2}{x^3} + \frac{15}{4x} + \frac{9}{5}x\right) + Qx^3\right], \qquad (40)$$

where $x = \sqrt{2/(s+1/s)}$ and Q was approximated by the rational function

TABLE II. The coefficients in Eq. (41).

i	p_i	q_i
0	−0.948874987216968	
1	5.20484573601241	−5.44950508637550
2	−6.62156460132033	7.74189993743446
3	−3.77999451107081	−1.40796939169607
4	0.441614216058416	8.63794384590824

$$Q = \frac{p_0 + p_1 x + p_2 x^2 + p_3 x^3 + p_4 x^4}{1 + q_1 x + q_2 x^2 + q_3 x^3 + q_4 x^4}. \tag{41}$$

The coefficients in Eq. (41) given in Table II were obtained by fitting the numerical values of $B_4^{[2f]}(s)$ with constraints given by Eqs. (36) and (37).

The agreement of expression Eq. (39) with the numerical results is shown in Fig. 5. The relative error of the semiemirical formula is less then 1.5×10^{-9}. Although it is about ten times greater than the differences for $B_4^{[1]}(s)$ and $B_4^{[3]}(s)$, the precision is more than sufficient for nearly all applications. We remark that the most precise existing semi-empirical formula due to Wheatley [31] has errors about million times greater.

IV. CONCLUSIONS

It previous sections, we calculated precisely the fourth virial coefficients of the additive hard-sphere mixture and found exact analytical formula for the partial virial coefficients $B_4^{[1]}(s)$ and $B_4^{[3]}(s)$ and very precise semiempirical formula for $B_4^{[2]}(s)$. The results obtained show that the fourth virial coefficient is not analytic at the diameter ratio $s = 2/\sqrt{3} - 1$. Using a similar argument we can prove that a similar nonanalycity must occur also for higher virial coefficients. Nearly all modern equations of state of the HS mixture are based on the modification of the scaled particle theory [32] (see [30] for a review) and they are analytical for all diameter ratios. Consequently, any attempt to improve substantially the equation of state must exhibit the same point of nonanalycity as the virial coefficients.

APPENDIX: THE CONTRIBUTIONS TO THE PARTIAL VIRIAL COEFFICIENTS

We used computer algebraic system Maple [29] to evaluate all but two-irreducible diagrams for $s < 1$

$$B_4^{[1a]} = -\frac{\pi^3}{90720}(5s^3 + 15s^2 - 147s + 263)(1 + s)^6, \tag{A1}$$

$$B_4^{[1b]} = \frac{\pi^3}{90720}(1575s^3 + 3078s^2 + 1431s + 263), \tag{A2}$$

$$B_4^{[1c]} = \frac{\pi^3}{181440}(10s^9 + 90s^8 + 36s^7 - 588s^6 - 504s^5 + 2520s^4 + 6300s^3 + 3780s^2 + 945s + 105), \tag{A3}$$

$$B_4^{[2a]} = -\frac{\pi^3}{22680}(25s^6 + 54s^5 - 297s^4 + 84s^3 + 1575s^2 + 630s + 105)s^3, \tag{A4}$$

$$B_4^{[2b]} = -\frac{17\pi^3}{90720}(1 + s)^9, \tag{A5}$$

$$B_4^{[2c]} = \frac{\pi^3}{181440}(100s^6 + 216s^5 - 1188s^4 + 756s^3 + 7875s^2 + 4095s + 840)s^3, \tag{A6}$$

$$B_4^{[2d]} = \frac{\pi^3}{90720}(420s^6 + 1575s^5 + 2142s^4 + 1428s^3 + 612s^2 + 153s + 17), \tag{A7}$$

$$B_4^{[2e]} = \frac{\pi^3}{90720}(17s^6 + 153s^5 + 612s^4 + 1428s^3 + 2142s^2 + 1575s + 420)s^3, \tag{A8}$$

$$B_4^{[3a]} = -\frac{\pi^3}{90720}(263s^3 - 147s^2 + 15s + 5)(1 + s)^6, \tag{A9}$$

$$B_4^{[3b]} = \frac{\pi^3}{90720}(263s^3 + 1431s^2 + 3078s + 1575)s^6, \tag{A10}$$

$$B_4^{[3c]} = \frac{\pi^3}{181440}(105s^9 + 945s^8 + 3780s^7 + 6300s^6 + 2520s^5 - 504s^4 - 588s^3 + 36s^2 + 90s + 10). \tag{A11}$$

[1] T. L. Hill, *Statistical Mechanics* (McGraw-Hill, New York, 1956).

[2] G. E. Uhlenbeck and G. W. Ford, in *Studies in Statistical Mechanics*, edited by J. de Boer and G. E. Uhlenbeck (North-Holland, Amsterdam, 1962).

[3] B. R. A. Nijboer and L. van Hove, Phys. Rev. **85**, 777 (1952).

[4] L. Boltzmann, Proc. Sect. Sci. K. Acad. Wet **7**, 484 (1899).

[5] M. N. Rosenbluth and A. W. Rosenbluth, J. Chem. Phys. **23**, 356 (1955).

[6] K. W. Kratky, Physica A **85**, 607 (1976).

[7] K. W. Kratky, Physica A **87**, 584 (1977).

[8] K. W. Kratky, J. Stat. Phys. **27**, 533 (1982).

[9] K. W. Kratky, J. Stat. Phys. **29**, 129 (1982).

[10] F. H. Ree and W. G. Hoover, J. Chem. Phys. **40**, 939 (1964).

[11] F. H. Ree and W. G. Hoover, J. Chem. Phys. **46**, 4181 (1967).

[12] E. J. J. van Rensburg and G. M. Torrie, J. Phys. A **26**, 943 (1993).

[13] E. J. J. van Rensburg, J. Phys. A **26**, 4805 (1993).

[14] A. Y. Vlasov, X.-M. You, and A. J. Masters, Mol. Phys. **100**, 3313 (2002).

[15] J. Kolafa, S. Labík, and A. Malijevský, Phys. Chem. Chem. Phys. **6**, 2335 (2004).

[16] N. Clisby and B. M. McCoy, J. Stat. Phys. **114**, 1361 (2004).

[17] T. Kihara, Rev. Mod. Phys. **27**, 412 (1955).

[18] T. Kihara and K. Miyoschi, J. Stat. Phys. **13**, 337 (1975).

[19] R. Blaak, Mol. Phys. **95**, 695 (1998).

[20] E. Enciso, N. G. Almarza, M. A. Gonzalez, and F. J. Bermejo, Phys. Rev. E **57**, 4486 (1998).

[21] F. Saija, G. Fiumara, and P. Giaquinta, Mol. Phys. **92**, 1089 (1997).

[22] R. Wheatley, F. Saija, and P. Giaquinta, Mol. Phys. **94**, 877 (1998).

[23] F. Saija, G. Fiumara, and P. Giaquinta, Mol. Phys. **87**, 991 (1996).

[24] K. D. Gibson and H. A. Scheraga, J. Phys. Chem. **91**, 4121 (1987).

[25] K. D. Gibson, J. Phys. Chem. **91**, 6326 (1987).

[26] S. Labík and W. Smith, Mol. Simul. **12**, 23 (1994).

[27] W. Smith and S. Labík, Mol. Phys. **80**, 1561 (1993).

[28] D. Matyushov and B. Ladanyi, J. Chem. Phys. **107**, 5815 (1997).

[29] M. B. Monagan, K. O. Geddes, K. M. Heal, G. Labahn, S. M. Vorkoetter, J. McCarron, and P. DeMarco, *Maple 9 Advanced Programming Guide* (Maplesoft, Waterloo, ON, 2003).

[30] C. Barrio and J. Solana, in *Theory and Simulation of Hard-Sphere Fluids and Related Systems*, Lecture Notes in Physics Vol. 753, edited by A. Mulero (Springer, Berlin, Heidelberg, 2008), pp. 133–182.

[31] R. Wheatley, J. Chem. Phys. **111**, 5455 (1999).

[32] H. Reiss, H. Frisch, and J. Lebowitz, J. Chem. Phys. **31**, 369 (1959).